Dynamic Behavior of Metal Vapor in Arc Plasma during TIG Welding†

TANAKA Manabu*, TASHISRO Shinichi, TSUJIMURA Yoshihiro*****

Abstract

In the present paper, the mechanism of metal vapor in arc plasma is discussed through the dynamic observation of spectra of helium, chromium, manganese and iron during stationary TIG welding of stainless steel. Wavelengths from 400 nm to 700 nm are observed by a monochromator with a diffraction grating. Radiation from the arc is sent to the monochromator through optical lens and spectroscopic images are captured with 500 fps by a high-speed digital video-camera. Spectra of metal elements exist locally in the arc plasma due to dependence of plasma temperature, and also intensive region of each metal spectrum depends on kinds of metal elements. The most part of metal vapor produced from the weld pool surface are carried on the cathode jet and then are swept away towards surroundings of the arc. However, if the driving force like diffusion in plasma is large, some metal elements can get across the cathode jet and then can be carried on the circulation flow towards tungsten electrode.

KEY WORDS: (Arc), (Plasma), (Metal vapor), (Spectroscopic analysis), (TIG), (Welding)

1. Introduction

Free-burning arcs are widely used in industrial applications, including arc welding [1], plasma splaying [2], plasma cutting [3] and so on. Many researchers have devoted experimental and theoretical efforts to understanding the physical characteristics of the arcs. These efforts helped to attain the practical understanding of the arc column and several books regarding arc physics have been published [4-6]. One of the practical understandings is effects of metal vapor. For example, metal vapor emanating from the electrodes contributes to self-stabilization of arcs and also to reduction of the anode fall, with the result that the arc voltage decreases. The presence of metal vapor in the arc is inevitable in the applications like arc welding because of the high temperature of the weld pool. The transport of metal vapor in the arc plasma is an important subject for investigation, since the vapor changes the arc properties, and therefore the properties of the weld pool. Many researchers had a variety of investigations of metal contaminated arc plasma [7-14]. Many studies on the effects of metal vapor have been reported and they make clear that the presence of metal vapor in the arc is important factor of the arc properties. However, experimental observations of process and diffusion for mixture of arc plasma and metal vapor from the weld pool are not reported.

In the present paper, spectroscopic analysis of helium and metal spectra is conducted in arc welding. The purpose of this paper is to make clear the mechanism of mixture of metal vapor in the arc plasma.

2. Experimental method

The TIG (Tungsten Inert Gas) arc is struck in pure helium atmosphere between a tungsten electrode and a flat stainless steel, SUS304, and then the stationary TIG welding is carried out for 20s after the arc ignition. The tungsten electrode is 3.2 mm in diameter and is ground to a conical tip angle of 60°. The TIG arc is operated at current of 150 A and the distance between electrodes is 3 mm.

Figure 1 shows a schematic drawing of spectroscopic analysis system for this study. Wavelengths from 400 nm to 700 nm can be observed by a monochromator. The monochromator is the Czerny-Turner type and has diffraction grating with wavelength resolution of 0.4 nm. Radiation from the arc is sent to the monochromator through optical lens and spectroscopic images are captured with 500 fps by

† Received on June 18, 2012
* Professor
** Assistant professor
*** Graduate Student

Transactions of JWRI is published by Joining and Welding Research Institute, Osaka University, Ibaraki, Osaka 567-0047, Japan

a high-speed digital video-camera (FACTCAM-512PCI, Photron). In this experiment, the spectra of HeI, CrI, MnI, FeI, CrII and FeII are observed. MnII spectrum was not able to be observed because of undetectable wavelength due to UV rays. The above wavelengths employed in this study are given in **Table 1** [15, 16].

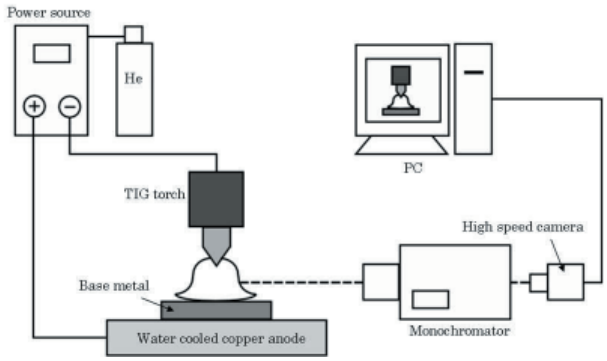

Fig. 1 Schematic drawing of spectroscopic analysis system

Table 1 Wavelengths of HeI, CrI, MnI, FeI, CrII and FeII spectral lines

Particle	Wavelength(nm)
Helium atom (He I)	587.6
Chromium atom (Cr I)	520.8
Manganese atom(Mn I)	476.2
Iron atom (Fe I)	538.3
Chromium ion (Cr II)	455.9
Iron ion (Fe II)	458.4

3. Observations at thermal plasma

Figures 2 to **5** show experimental results of spectroscopic images of HeI, CrI, MnI and FeI spectra. Intensity of HeI spectrum weakens with passing time. Table 2 shows excitation energies of each spectrum [18] and **Figure 6** shows the dependence of normalized radiant intensities on temperature [18, 19]. Excitation energy of HeI is the very highest in **Table 2** and temperature region for emission of HeI spectrum is much higher than other spectra. Temperature of plasma becomes lower due to effects of metal vapor which has generally low excitation energies. Therefore, the helium is not able to be excited, and the bright region of HeI shrinks and then disappears at 19s after arc ignition.

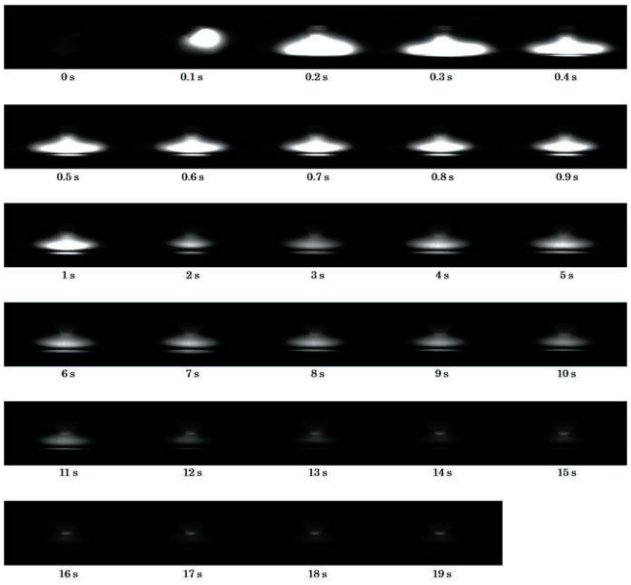

Fig. 2 Photographs of HeI spectrum in arc during helium TIG welding of stainless steel

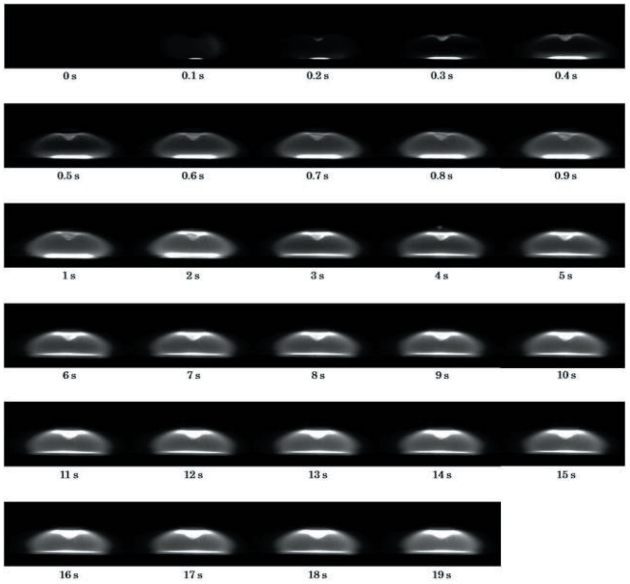

Fig. 3 Photographs of CrI spectrum in arc during helium TIG welding of stainless steel

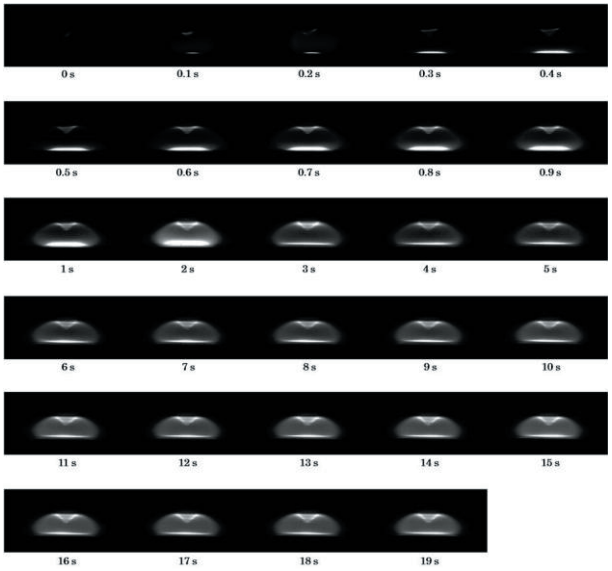

Fig. 4 Photographs of MnI spectrum in arc during helium TIG welding of stainless steel

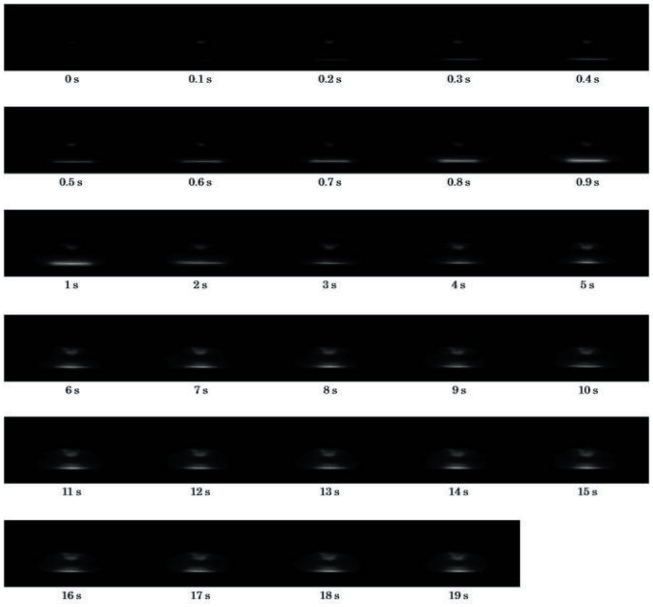

Fig. 5 Photographs of FeI spectrum in arc during helium TIG welding of stainless steel

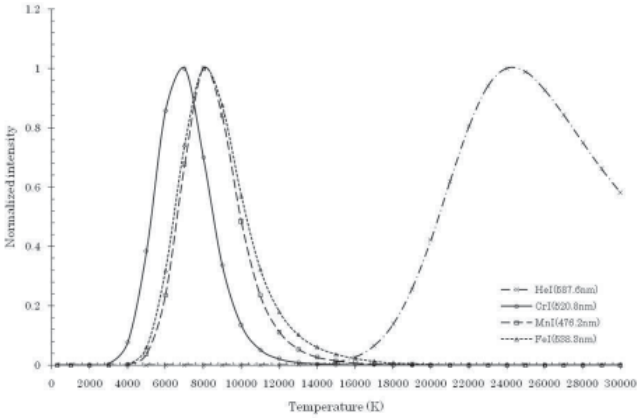

Fig. 6 Dependence of normalized radiant intensities on temperature for spectra of HeI, CrI, MnI and FeI

Table 2 Excitation energies of HeI, CrI, MnI and FeI particles

Particle	Excitation energy (eV)
HeI 587.6nm	23.07
CrI 520.8nm	3.32
MnI 476.2nm	5.49
FeI 538.3nm	6.61

Spectra of CrI, MnI and FeI do not exist in the arc plasma in the same manner. Intensities of CrI and MnI spectra are very strong in the arc column, but FeI spectrum can be observed only close to the weld pool surface. It is suggested that existential location of metal vapor in the arc plasma depends on kinds of metal elements. It is also expected that chromium and manganese exist inside the arc plasma, but iron is swept away toward the surroundings of the arc plasma.

4. Observations at electrodes

Figure 7 shows analytic results of elemental mapping of the tungsten electrode by the FE-SEM after the stationary TIG welding of stainless steel for 20s. A lot of chromium exists on the surface of tungsten electrode at about 1.7 mm and over from the tungsten electrode tip. Manganese and iron are not able to be detected and it is negligible.

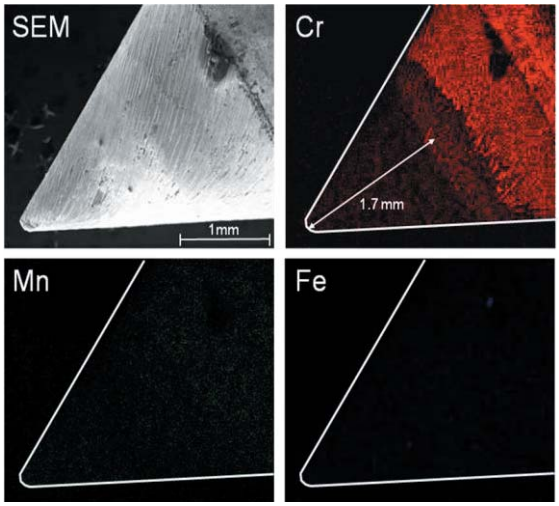

Fig. 7 Results of elemental analysis of the tungsten electrode after TIG welding of stainless steel for 20s

A two-color pyrometry with a high-speed digital video-camera has been conducted to obtain the surface temperature of tungsten electrode [20]. **Figure 8** shows axial temperature distribution of tungsten electrode. Boiling points of chromium, manganese and iron are 2933 K, 2305 K, and 3160 K, respectively [18]. Surface temperature of tungsten electrode is about 3500 K at the tungsten electrode tip and is reduced by 3000 K at 1.7 mm from the tip as shown in Fig. 8. From a comparison of the boiling point of chromium and the result of Fig. 8, chromium exists where a surface temperature of tungsten electrode is under the boiling point. However, manganese can hardly exist because of low boiling point. Although surface temperature of tungsten electrode becomes lower than the boiling point of iron (about 3200 K) at about 1.6 mm and over from the tip, iron has not the same tendency with chromium. From these results, it can be concluded that there is few iron vapor inside the arc plasma.

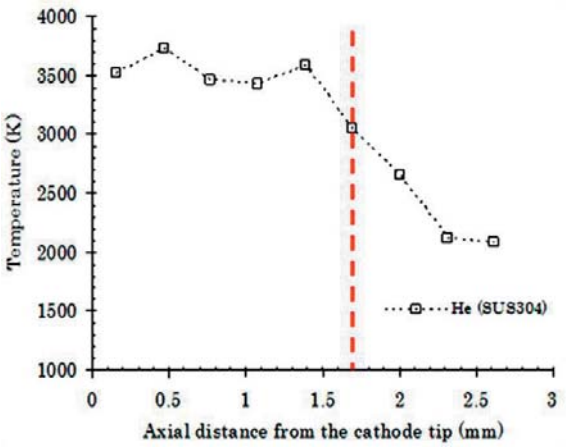

Fig. 8 Axial temperature distribution of tungsten electrode during TIG welding of stainless steel

On the other hand, smut on the stainless steel after the stationary TIG welding is analyzed quantitatively. **Figure 9** shows results of quantitative analysis of the smut by the EDAX (Energy Dispersive Analysis of X-ray). The smut consists of a lot of manganese and iron which are hardly detected on the surface of tungsten electrode, and also consists of a little of chromium.

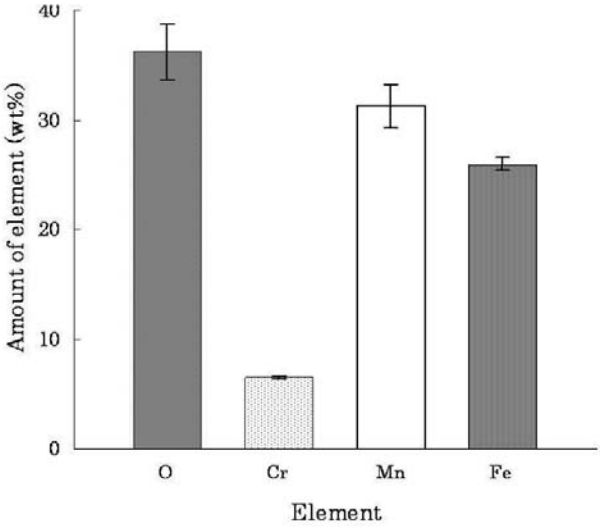

Fig. 9 Result of quantitative analysis of smut by EDAX after TIG welding of stainless steel for 20s

5. Discussion

In TIG arc, current density at the tungsten cathode tip is much higher than on the base metal, and then a strong plasma fluid flow from cathode to anode, i.e., the cathode jet occurs [21]. The most part of metal vapor from the weld pool surface are swept away towards surroundings of the arc plasma by the cathode jet.

Calculation result of Ushio [22] show that arc plasma has not only the cathode jet but also a convective circulation flow. It is suggested that a part of metal vapor can be carried on this circulation flow towards tungsten electrode. And then, the metal vapor can transport into the arc column, as shown in Fig. 10.

Diffusion of metal vapor in plasma is one of driving forces to lead metal vapor into the arc plasma. Diffusion of metal vapor in plasma [23] is given by the following equation,

$$\overline{J_A} = \frac{n^2}{\rho}\overline{m_A}\,\overline{m_B}\left(\overline{D_{AB}^{x}}\nabla\overline{x_B} + \overline{D_{AB}^{E}}E\right) - \overline{D_{AB}^{T}}\nabla\ln T \tag{1}$$

where, n and ρ are respectively the number density and mass density of gas, E is the electrical field, T is the temperature, $\overline{m_A}$ and $\overline{m_B}$ are

respectively the average mass of the heavy particle of gas A and gas B, $\nabla\overline{x_B}$ is the sum of mole fractions of all species of gas B, $\overline{D^x_{AB}}$, $\overline{D^E_{AB}}$ and $\overline{D^T_{AB}}$ are respectively the combined diffusion coefficients for ordinary, electrical field and thermal diffusion. The first term shows ordinary diffusion by concentration gradient, the second term shows diffusion by potential gradient, and the third term shows diffusion by temperature gradient. The diffusion by temperature gradient is small and then negligible in low temperature region like a weld pool surface [24]. Diffusion coefficient of metal element increases with increase of concentration of metal element, and metal vapor becomes easy to diffuse. Large amount of manganese can evaporate because of its lower boiling point. Therefore, diffusion by concentration gradient has the most effect for manganese vapor in other metal elements. Ionization energies of chromium, manganese and iron are 6.77 eV, 7.43 eV, and 7.90 eV, respectively. The ionization energy of chromium is about 0.7~1.1 eV smaller than other metal elements. In particularly low temperature plasma which is close to the weld pool surface, chromium would be preferentially ionized in comparison with manganese and iron. Therefore, it is considered that diffusion by potential gradient has the most effect for chromium vapor.

In the TIG arc, there is not only the cathode jet but also a convective circulation flow, as shown in **Fig. 10**[22]. This convective circulation flow is an upper stream in comparison with the cathode jet on the weld pool surface. The most parts of metal vapor produced from the weld pool surface are swept away to surroundings of the arc plasma by the cathode jet. However, some parts of metal vapor are affected by a driving force like the diffusion. If the driving force by the diffusion is so large, some metal elements can get across the cathode jet and can reach the circulation flow which is situated on the upper stream of the cathode jet, and then these metal elements are carried on the circulation flow towards tungsten electrode. It is thought that vapors of chromium and manganese can mix in the arc plasma through the circulation flow due to the diffusion on the weld pool surface. Dominant driving forces of the diffusion are the concentration gradient for manganese and the potential gradient for chromium. However, iron vapor is not able to diffuse into the circulation flow across the cathode jet and then is swept away towards surroundings of the arc plasma by the cathode jet, because iron vapor is low concentration in arc plasma close to the weld pool surface due to higher boiling point and also there are hardly ions of iron in arc plasma close to the weld pool surface due to higher ionization energy.

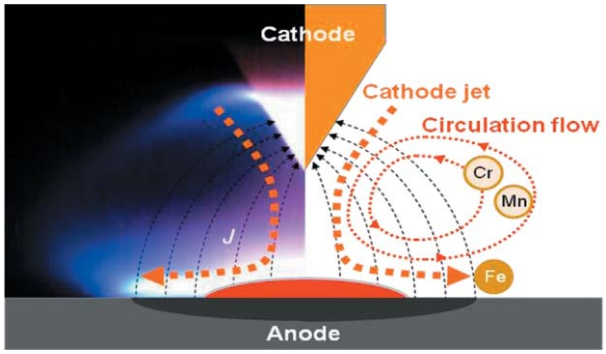

Fig. 10 Illustration of convective circulation flow in TIG arc

6. Conclusions

The conclusions of this work are summarized as follows.

(1) Intensity of HeI spectrum weakens with passing time. It is because temperature of plasma becomes lower due to metal vapor in the arc plasma.

(2) Large amount of manganese and chromium vapor exist in the arc plasma. However, few amount of iron vapor exist in the arc plasma.

(3) Chromium is easy to diffuse by potential gradient due to its lower ionization energy and chromium vapor from the weld pool surface mix in the arc plasma through a convective circulation flow in the arc.

(4) Large number of manganese can evaporate due to its lower boiling point. Therefore, manganese is easy to diffuse by concentration gradient and manganese vapor from the weld pool surface can mix in the arc plasma through a convective circulation flow in the arc.

(5) Iron vapor from the weld pool surface is swept away towards surroundings of the arc plasma by the cathode jet, because driving force of iron to diffuse is too weak to mix in the arc plasma due to its higher boiling point and also higher ionization energy.

References

1) M. Tanaka and J.J. Lowke: Predictions of weld pool profiles using plasma physics, J. Phys. D: Appl. Phys., 40 (2007), pp. R1-R24.

2) P. Fauchais: Understanding plasma spraying, J. Phys. D: Appl. Phys., 37 (2004), pp. R86-R108.

3) V.A. Nemchinsky and R. Severance: What we know and what we do not know about plasma cutting, J. Phys. D: Appl. Phys., 39 (2006), pp.R423-R438.

4) M.N. Hirsh and H.J. Oskam: Gaseous Electronics, 1978, Academic Press, New York.

5) J.F. Lancaster : Physics of Welding, 1984, Pergamon Press, Oxford.

6) M.I. Boulos, P. Fauchais and E. Pfender: Thermal Plasmas, 1994, Plenum Press, New York.

7) K. Etemadi and E. Pfender: Impact of Anode Evaporation on the Anode Region of High-Intensity Argon Arc, Plasma Chem. Plasma Proc., 5 (1985), pp. 175-182.
8) G.J. Dunn, C.D. Allenmand and T.W. Eagar: Metal Vapors in Gas Tungsten Arcs: Part I. Spectroscopy and Monochromatic Photography, Metall. Trans., A, 17A (1986), pp.1851-1863.
9) G.J. Dunn and T.W. Eagar: Metal Vapors in Gas Tungsten Arcs: Part II. Theoretical Calculations of Transport Properties, Metall. Trans., A, 17A (1986), pp.1865-1871.
10) A.J.D. Farmer, G.N. Haddad and L.E. Cram: Temperature determinations in a free-burning arc: III. Measurements with molten anodes, J. Phys. D: Appl. Phys., 19 (1986), pp. 1723-1730.
11) K. Yamamoto, M. Tanaka, S. Tashiro, K. Nakata, K. Yamazaki, E. Yamamoto, K. Suzuki and A.B. Murphy: Metal vapour behavior in thermal plasma of gas tungsten arcs during welding, Sci. Technol. Weld. Joining, 13 (2008), pp. 566-572.
12) A.B. Murphy, M. Tanaka, K. Yamamoto, S. Tashiro, T. Sato and J.J. Lowke: Modelling of thermal plasma for arc welding: the role of the shielding gas properties and of metal vapour, J. Phys. D: Appl. Phys., 42 (2009), p.194006.
13) M. Schnick, U. Fussel, M. Hertel, A. Spille-Kohoff and A.B. Murphy: Metal vapour causes a central minimum in arc temperature in gas-metal arc welding through increased radiative emission, J. Phys. D: Appl. Phys., 43 (2010), p. 022001.
14) M. Tanaka, K. Yamamoto, S. Tashiro, K. Nakata, E. Yamamoto, K. Yamazaki, K. Suzuki, A.B. Murphy and J.J. Lowke: Time-dependent calculations of molten pool formation and thermal plasma with metal vapour in gas tungsten arc welding, J. Phys. D: Appl. Phys., 43 (2010), p. 434009.
15) S. Zielinska, K. Musiol, K. Dzierzega, S. Pellerin, F. Valensi, Ch de Izarra and F. Briand, Investigation of GTAW plasma by optical emission spectroscopy, Plasma Sources Sci. Technol., 16 (2007), pp. 832-838.
16) W.L. Wiese, M.W. Smith and B.M. Miles: Atomic Transition Probabilities, 1966, NSRDS, National Standard Reference Data Series, Washington.
17) H. Terasaki, M. Tanaka and M. Ushio: Effects of metal vapor on electron temperature in helium gas tungsten arcs, Metall. & Mater. Trans. A, 33A (2002), pp.1183-1188.
18) The Japan Institute of Metals: Data Book of Metals, 1993, Maruzen, Tokyo.
19) National Institute of Standards and Technology (NIST): Atomic Spectra Database, 2008
http://www.nist.gov/pml/data/asd.cfm
20) S. Tashiro and M. Tanaka: Effect of admixture of metal vapor on cathode surface temperature of plasma torch, Surface and Coating Technology, 202 (2008), pp. 5255-5258.
21) M. Tanaka and M. Ushio: Plasma state in free-burning argon arc and its effect on anode heat transfer, J. Phys. D: Appl. Phys., 32 (1999), pp.1153-1162.
22) M. Ushio and F. Matsuda: A Mathematical Modeling of flow and Temperature Fields in Gas-Tungsten-Arc, Quarterly J. of Japan Weld. Society, 6 (1988), pp.91-98.
23) A.B. Murphy: Cataphoresis in electric arcs, J. phys. D: Appl. Phys., 31 (1998), pp.3383-3390.
24) A.B. Murphy: A comparison of treatments of diffusion in thermal plasmas, J. phys. D: Appl. Phys., 29 (1996), pp.1922-1932.